Karami-Horestani, Amirhossein; Paredes, Ferran; Martín, Ferran. «Phase-Variation Microwave Displacement Sensor With Good Linearity and Application to Breath Rate Monitoring». IEEE sensors journal, Vol. 23, Issue 19 (October 2023), p. 22486-22495. DOI 10.1109/JSEN.2023.3307575

Phase-Variation Microwave Displacement Sensor with Good Linearity and Application to Breath Rate Monitoring

Amirhossein Karami-Horestani, *Member, IEEE,* Ferran Paredes, *Senior Member, IEEE,* and Ferran Martín, *Fellow, IEEE*

***Abstract*—This paper presents a novel highly linear reflective-mode displacement sensor based on planar microwave technology. The sensor consists of two parts: (i) the stator, or reader, a one-port transmission line terminated with a matched load, and (ii) the movable part, or tag, a dielectric slab with an electric LC (ELC) resonator etched on it. In the proposed system, the resonator is allowed to displace longitudinally along the line axis of the reader at a fixed vertical distance (air gap). Due to magnetic coupling between the line and the ELC resonator, the feeding signal (a harmonic signal tuned to the resonance frequency of the ELC resonator) is totally reflected at the resonator's position, and the phase of the reflection coefficient, the output variable of the sensor, correlates with that position, i.e., it varies roughly linearly with the distance between the resonator and the input port. A prototype example, with a dynamic range of 4.40 cm, is reported, and validated at laboratory level by means of a linear displacement system. Then, the potential of the proposed sensor to monitoring the breath rate in humans is discussed, and a belt-based prototype device system that can be applied for that purpose is presented and validated. The key idea is the chest and abdomen expansion due to breathing, which leads to a periodic relative displacement between the tag and the reader at the respiration rate.**

***Index Terms*— Breath rate monitoring, displacement sensor, microstrip technology, microwave sensor, phase-variation sensor, reflective-mode sensor.**

I. Introduction

THERE ARE various microwave techniques for the measurement of short-range linear and angular displacements [1]. One of such techniques is based on the variation of the resonance frequency caused by a relative displacement (linear or angular) between the movable part of the sensor (where a resonant element is etched), and the static part, implemented by means of a transmission line-based structure [2]-[4]. The main limitative aspect of such sensors concerns the fact that a wideband interrogation signal, at least covering the output dynamic range, is required for sensing, and this represents a penalty in terms of cost of the associated electronics.

The previous limitation of frequency-variation sensors is alleviated by considering the so-called single-frequency sensors, where the sensing device (in operational environment) should be fed by a single-tone (harmonic) interrogation signal. Such signal can be generated by means of a simple harmonic oscillator, or by means of a narrow-band (and low cost) voltage-controlled oscillator (VCO) tuned to a certain frequency. Single-frequency sensors can be divided in two main groups, i.e., coupling modulation sensors and phase variation sensors. Coupling modulation sensors have been mostly applied to the measurement of linear and angular displacements and velocities [5]-[12], whereas phase-variation sensors have been mainly focused on the measurement of material properties [13]-[30] (nevertheless, examples of phase-variation sensors devoted to the measurement of short-range linear and angular displacements have been reported [31]-[34]).

In coupling modulation sensors, a resonant element (or various resonant elements) in relative motion with regard to the static part (typically a transmission line) modify the transmission (in transmission-mode sensors) or reflection (in reflective-mode sensors) coefficient, and particularly its magnitude at the operating frequency (the output variable). In most of these coupling-modulation displacement sensors, the dynamic range is of the order of the dimensions of the considered sensing resonators. Nevertheless, there is a type of coupling modulation sensors that exhibits long range (i.e., high input dynamic range) measurements, i.e., the so-called electromagnetic (or microwave) encoders [35]-[38]. Such devices are based on chains of inclusions (not necessarily resonators) etched or printed on a dielectric substrate, and such

This work was supported by MCIN/AEI 10.13039/501100011033, Spain, through the projects PID2019-103904RB-I00 (ERDF European Union) and PDC2021-121085-I00 (European Union Next Generation EU/PRTR), by the AGAUR Research Agency, Catalonia Government, through the project 2021SGR-00192, and by Institució Catalana de Recerca i Estudis Avançats (who awarded Ferran Martín). A. Karami-Horestani acknowledges MCIN/AEI /10.13039/501100011033 and ESF for Grant PRE2020-093239.

A. Karami-Horestani, F. Paredes, and F. Martín are with GEMMA/CIMITEC, Departament d'Enginyeria Electrònica, Universitat Autònoma de Barcelona, 08193 Bellaterra, Spain. (e-mail: Amirhossein.Karami@uab.cat).

chains are either linear (in linear encoders) or circular (in rotary encoders). As the encoder (or tag) moves on top of the reader (a transmission line) at short distance, the inclusions of the chain perturb the transmission coefficient each time an inclusion lies on top of the reader line, thereby modulating the amplitude of the harmonic signal injected to the input port of the reader line. Thus, pulses in the envelope function, which can be retrieved by means of an envelope detector, are generated. The time lapse between adjacent pulses provides the instantaneous velocity, whereas the cumulative number of pulses gives the linear or angular displacement from a reference position. Actually, this is the working principle of the so-called incremental encoders. However, quasi-absolute encoders, where at least one chain is equipped with a certain identification (ID) code, have been reported [39]-[47]. The main advantage of such quasi-absolute encoders over incremental-type encoders is the possibility of determining the encoder position after a system reset (without the need to return to the reference position).

Coupling-modulation displacement sensors essentially exploit the magnitude of the reflection or transmission coefficient at a certain frequency. Such magnitude can be easily converted to a voltage, a measurable magnitude. There are also displacement sensors that exploit both the magnitude and frequency of the sensor response. One example is constituted by a set of recently reported rotation sensors based on single interference techniques [48]-[51]. Such sensors exhibit a reasonable performance (sensitivity), but like frequency-variation sensors, they need wideband signals for sensing.

We should mention that magnitude measurements are more prone to the effects of electromagnetic interference (EMI) and noise, as compared to frequency or phase measurements. Therefore, it follows that phase-variation sensors benefit from the advantages of single-frequency measurements (low cost of the associated electronics in real environment) and the robustness against EMI and noise, inherent to phase measurements. Nevertheless, despite the advantages of phase-variation sensors over frequency-variation and coupling-modulation sensors, few works have been dedicated to exploit such advantageous aspects for the implementation of displacement sensors. Among them, in [32], [33] angular displacement sensors based on rotatable resonators that vary the phase of the reflection or transmission coefficient when they rotate, are reported. In [31], a linear displacement sensor, based on a step-impedance configuration and a movable dielectric slab was reported. The sensitivity in such sensor is very good, but at the expense of a limited linearity and input dynamic range. In a very recent work [34], the authors report a rotation sensor based on a coplanar waveguide (CPW) terminated with a circular step-impedance resonator, where the movable part is a circularly shaped dielectric slab. This sensor exhibits reasonably good sensitivity and linearity, the later achieved by tapering the step-impedance resonator.

In this paper, we propose a reflective-mode phase-variation linear displacement sensor, where the main target is the linearity. The sensor operates under a principle radically different to the one used in [31], where the target was to achieve very good sensitivity at the expense of linearity. That is in [31], like in [34], a movable dielectric slab modifies the phase of the reflection coefficient when it displaces over the sensitive part of the sensor at short vertical distance. In this paper, the sensitive part of the reader is a transmission line terminated with a matched load, whereas the movable part is a resonator (an electric LC –ELC– resonator) etched on a dielectric slab. As the resonator displaces along the line axis at short vertical distance, the phase of the reflection coefficient varies quasi-linearly, as desired.

The paper is organized as follows. The proposed displacement sensor and its working principle, including a sensitivity analysis, are presented in Section II. In Section III, the sensor is validated both at simulation level and experimentally by considering a linear displacement system available in our laboratory. In Section IV, the potentiality of the reported sensor as a device able to retrieve the breath rate is discussed, and a second prototype, based on a stretchable belt is designed and fabricated to experimentally validate the approach. A comparison with other displacement sensor and breath rate sensors is the subject of Section V. Finally, the main concluding remarks are highlighted in Section VI.

II. Sensor concept and analysis

The perspective view of the sensor (a sketch including the static and movable parts) is depicted in Fig. 1(a). The static part, or reader, merely consists of a transmission line terminated with a matched load feed by a harmonic (single tone) signal. The movable part, or tag, is an ELC resonator [52] etched in a dielectric slab. For sensor functionality, the ELC resonator must be displaced along the line axis of the reader with the magnetic wall at the fundamental resonance aligned with the line axis [Fig. 1(b) depicts the topology of the ELC resonator with indication of the currents, as well as the magnetic wall at the fundamental resonance]. With this relative orientation between the resonator and the line, the counter magnetic fields generated by the line in the two loops of the ELC resonator excite the particle, resulting in a strong magnetic coupling between the line and the resonant element. Nevertheless, for particle excitation, it is necessary that the frequency of the feeding signal coincides with the fundamental resonance frequency of the ELC resonator.

The line loaded with the ELC resonator can be modelled as depicted in Fig. 2, where l_1 is the distance between the resonator and the input port, and l_2 is the distance between the resonator and the matched end of the line (so that the total length of the line is $l = l_1 + l_2$). Note that the magnetic coupling between the line and the resonant element is equivalent to series connecting a parallel resonator to the line [53], [54] (losses are neglected in the model). If the injected harmonic signal is tuned to the resonance frequency of the ELC resonator, an open circuit in the resonator's plane arises, and the reflection coefficient is [55]

$$\rho = e^{-2j\phi_1} \qquad (1)$$

provided the characteristic impedance of the line is identical to that of the port ($Z_c = Z_0$), as indicated. Consequently, the phase of the reflection coefficient is

$$\phi_\rho = -2\phi_1 = -2\beta l_1 \quad (2)$$

where $\phi_1 = \beta l_1$ is the electrical length of the transmission line section present between the input port and the resonator position, and β is the phase constant of the line.

According to (2), the phase of the reflection coefficient varies linearly with the distance l_1. Consequently, the relative displacement between the resonator position and the input port can be measured. With $Z_c = Z_0$, and the opeating frequency set to f_0 (the fundamental resonance frequency of the ELC resonator), the sensor is expected to exhibit good linearity. Indeed, the sensitiviy, or derivative of the output signal with regard to the input signal is simply

$$\frac{d\phi_\rho}{dl_1} = -2\beta \quad (3)$$

i.e., a constant value.

Let us assume that to unambiguously determine the displacement, a unique cycle in the output variable is considered, i.e., $0 < \phi_\rho < 2\pi$. This means that the maximum displacement $l_{1,\max}$ should correspond to an electrical length of $\phi_{1,\max} = \pi$, according to (2). Thus, the input dynamic range is comprised in the range $0 < l_1 < \pi/\beta = l_{1,\max}$, the maximum displacement given by

$$l_{1,\max} = \frac{\pi}{\omega_0} v_p = \frac{c}{2f_0\sqrt{\varepsilon_{\rm eff}}} \quad (4)$$

From (4), it follows that input dynamic range is inversely proportional to the operating frequency. Moreover, it is convenient to deal with low dielectric constant substrates, provided the interest is to enhance the input dynamic range. In (4), ω_0 is the angular operating frequency, c is the speed of light in vacuum, and $\varepsilon_{\rm eff}$ is the effective dielectric constant (which decreases as the substrate dielectric constant decreases). To gain insight on the typical values of the input dynamic range, let us assume that the operating frequency is set, for example, to $f_0 = 1$ GHz, and that the effective dielectric constant is $\varepsilon_{\rm eff} = 4$. Introduction of these values in (4) gives $l_{1,\max} = 7.5$ cm (a reasonable value for the intended application, i.e., monitoring the breath rate, as will be later discussed).

III. Prototype Linear Displacement Sensor

Let us next report the first designed and fabricated prototype sensor aimed to the measurement of short range (i.e., few cm) displacements. The reader is implemented in the *Rogers 4003C* substrate with dielectric constant $\varepsilon_r = 3.55$, thickness $h = 0.81$ mm and loss tangent tanδ = 0.0022. The considered air gap between the reader and the movable resonator, etched in an identical substrate, is $g = 1$ mm. With this cross section, the width of the reader line necessary to achieve a characteristic impedance of $Z_c = Z_0 = 50$ Ω is $W = 1.8$ mm. The effective dielectric constant of such line, with the resonator substrate on top of it at 1 mm distance has been estimated to be $\varepsilon_{\rm eff} = 2.77$. We have set the operating frequency at $f_0 = 2.00$ GHz. Thus, according to (4), the maximum displacement is $l_{1,\max} = 4.40$ cm.

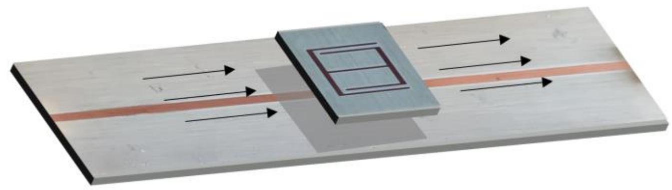

(a)

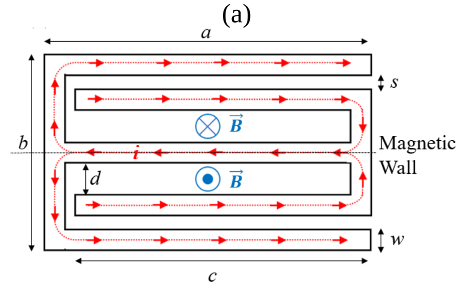

(b)

Fig. 1. Perspective view of the proposed reflective-mode phase-variation displacement sensor (a), and topology of the ELC resonator (b).

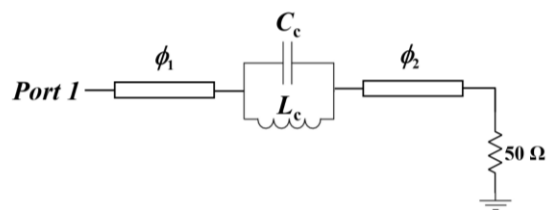

Fig. 2. Equivalent circuit model of the ELC loaded transmission line terminated with a matched load.

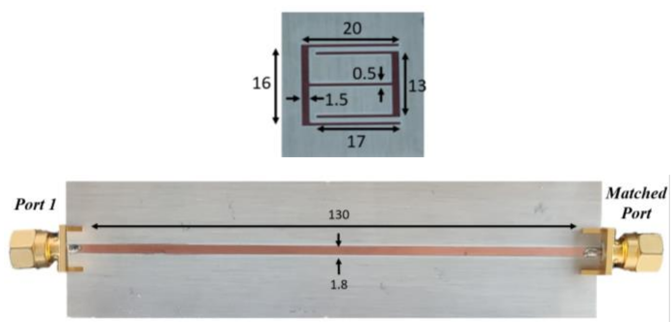

Fig. 3. Photograph of the fabricated reader and resonator with their dimensions in mm.

We have designed the ELC resonator in order to exhibit its fundamental resonance at f_0. The specific dimensions of the ELC resonator that provides such resonance frequency are given in Fig. 3. Note that the resonator exhibits a rectangular geometry. The side parallel to the line axis should not be too long, in order to have a small electrical length for the resonator in the direction of the line axis. This is important to faithfully assign a position to the resonator. Figure 3 depicts the photograph of the fabricated reader and resonator (for fabrication, the *LPKF H100* drilling machine has been used). The length of the reader line has been set to 13 cm, a value higher than the input dynamic range (nevertheless, we restrict the motion to a maximum displacement of $l_{1,\max} = 4.40$ cm).

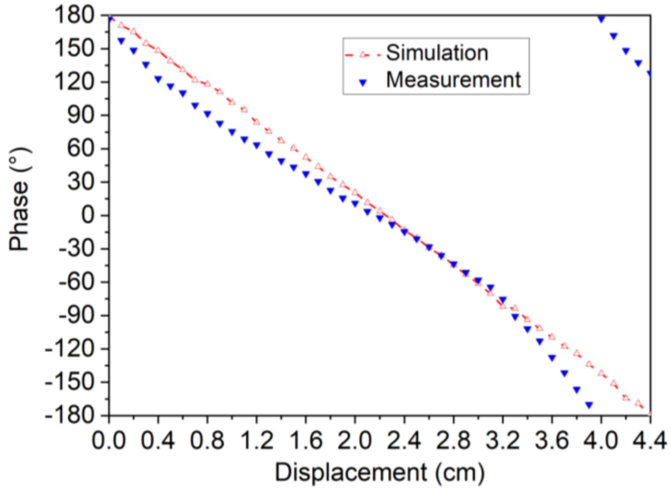

Fig. 4. Variation of the phase of the reflection coefficient with the displacement as inferred from electromagnetic simulation and measurement.

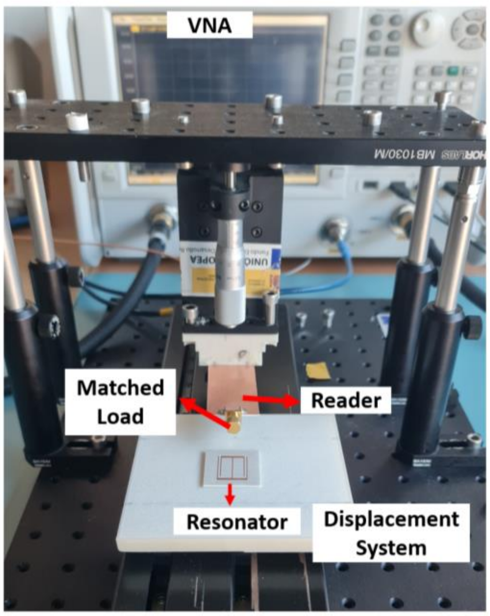

Fig. 5. Photograph of the experimental setup.

The phase of the reflection coefficient at f_0 as the ELC resonator is displaced along the line, on top of it with the indicated air gap distance, was inferred from full-wave electromagnetic simulation. For that purpose, the *ANSYS HFSS* commercial software was used. The input dynamic range was restricted to a length corresponding to $l_{1,\max}$ = 4.40 cm. The results are depicted in Fig. 4 and referenced to the phase of the reflection coefficient corresponding to the initial position of the ELC resonator. According to the figure, the phase of the reflection coefficient varies linearly, as expected, and the output dynamic range is 2π (corresponding to a complete cycle). The setup for the measurement of the phase of the reflection coefficient at f_0, as the resonator moves on top of the line, is depicted in Fig. 5. The reflection coefficient was retrieved by means of the vector network analyzer, model *Agilent N5221A*. For tag motion, the linear displacement system model *Thorlabs LTS300/M*, available in our laboratory, was used (the air gap was adjusted to the nominal value of g = 1 mm). The measured phase of the reflection coefficient at f_0 is also depicted in Fig. 4, and the agreement with the simulations is reasonably good. The average sensitivity, as inferred from the measured phase response, is found to be 8.2º/mm, in good agreement with (3) [with the estimated value of the phase constant, β, expression (3) provides a sensitivity of 8.0º/mm]. With these results, the sensor functionality is validated.

IV. Sensor System for Monitoring the Breath Rate

The phase-variation displacement sensor concept (experimentally validated in the previous section), conveniently modified, can be applied to the measurement of the breath rate. The breath rate sensor consists of a belt that must be adjusted to the abdomen or thorax of the individual under test (or subject under test –SUT– from now on), see Fig. 6. The belt has a stretchable part that elongates during the inspiration and constrains during the expiration. This means that the total length of the belt varies according to the abdominal or thoracic perimeter of the SUT, modulated by the respiration process. The reader is placed in the non-stretchable part of the belt and should contain a pair of rails in order to guide the movable part (where the board with ELC resonator etched on it is placed) over it at short distance (air gap). One end of the movable part is attached to part of the belt on the other side of the stretchable fabric, so that a relative quasi-periodic movement between the reader and the tag, dictated by the respiration rate, is expected. Figure 7 depicts a sketch of the belt and indicates how the relative motion between the reader and the tag proceeds by respiration.

For the implementation of the prototype breath rate sensor, the same reader used in the validation of the previous section was used. However, rails made with a 3D-printer (model Ultimaker 3 extended) were attached in order to guide the resonator over the reader at short distance. The resonator was implemented on the dielectric substrate (*Rogers 4003C*), with dielectric constant ε_r = 3.55, thickness h = 0.81 mm, and loss tangent tanδ = 0.0022. The photograph of the fabricated belt, including the reader and the tag, is depicted in Fig. 8.

For experimental validation, the belt was adapted to a volunteer, who was asked to breath three times normally and three times deeply. The phase of the reflection coefficient was recorded using VNA by data logging every 0.1 s. The recorded data is depicted in Fig. 9 and. As it can be seen, the breath rate of the volunteer can be easily extracted.

In the experimental results of Figs. 4 and 9, the phase of the reflection coefficient was retrieved by means of a VNA. Let us next consider a system closer to operational environment, by replacing the VNA with a microwave circuitry (a coupler pair), a gain/phase detector, and a microcontroller. The sketch of the proposed system can be seen in Fig. 10, where the interconnection of such components can be appreciated. The details of this system to retrieve the phase of the reflection coefficient are detailed in a recent paper [29], and hence are not repeated here. The feeding signal in real operation should be generated by means of a VCO. Nevertheless, we have fed the

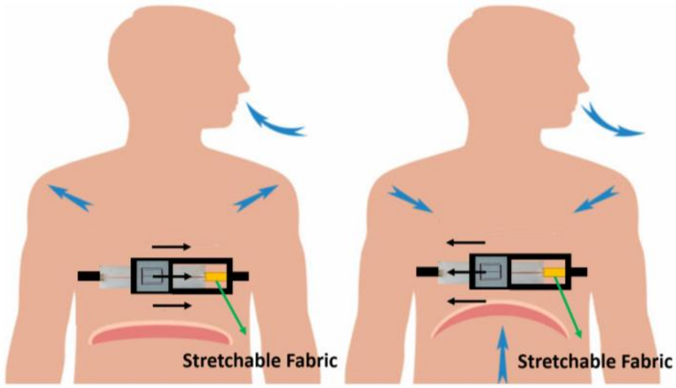

Fig. 6. Breath rate sensor concept.

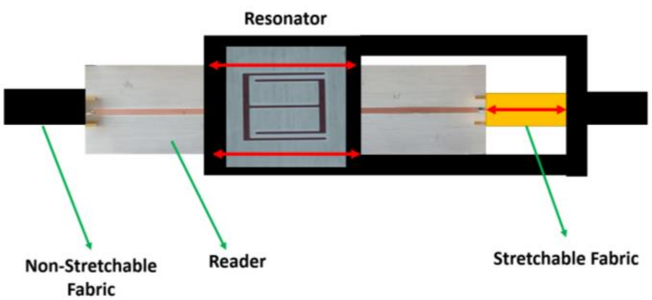

Fig. 7. Sketch of the belt with indication of the working principle.

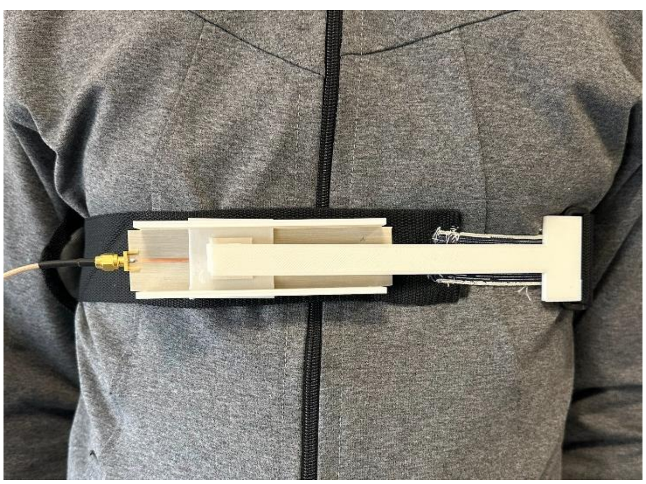

Fig. 8. Photograph of the fabricated breath rate belt sensor.

system with a VNA (with this sole purpose) in this paper. Using the setup of Fig. 10, we first measured the phase of the reflection coefficient at f_0 as a function of the displacement of the tag. The results are shown in Figure 11. Then we measured the breath rate by adapting the mentioned belt-based sensor to a volunteer, who, again, was asked to breath three times normally, and three times intensively (the results are depicted in Fig. 12).

In the experimental results of Figs. 4 and 9, the phase of the reflection coefficient was retrieved by means of a VNA. Let us next consider a system closer to operational environment, by replacing the VNA with a microwave circuitry (a coupler pair), a gain/phase detector, and a microcontroller. The sketch of the proposed system can be seen in Fig. 10, where the

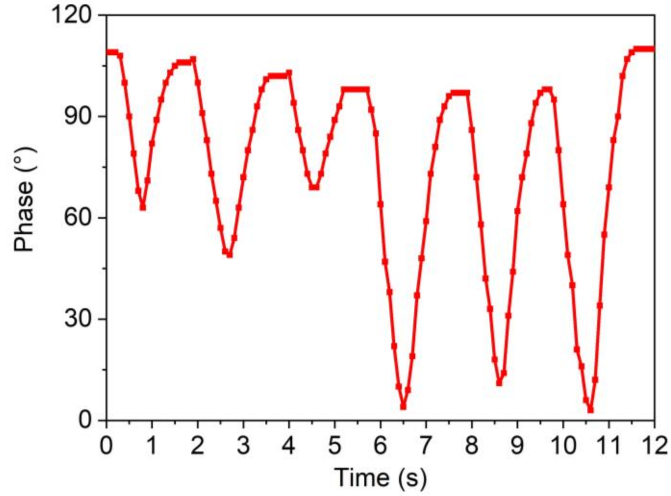

Fig. 9. Phase of the reflection coefficient recorded using a VNA while a volunteer wearing the belt-based sensor breaths as indicated in the text.

interconnection of such components can be appreciated. The details of this system to retrieve the phase of the reflection coefficient are detailed in a recent paper [29], and hence are not repeated here. The feeding signal in real operation should be generated by means of a VCO. Nevertheless, we have fed the system with a VNA (with this sole purpose) in this paper. Using the setup of Fig. 10, we first measured the phase of the reflection coefficient at f_0 as a function of the displacement of the tag. The results are shown in Figure 11. Then we measured the breath rate by adapting the mentioned belt-based sensor to a volunteer, who, again, was asked to breath three times normally, and three times intensively (the results are depicted in Fig. 12).

It should be mentioned that due to the nonlinear behaviour of the gain/phase detector, and to the fact that the input impedances of the gain/phase detector are not matched at f_0, the usable range in which the phase of the reflection coefficient varies linearly with the displacement is roughly 3 cm, rather than 4.4 cm. Note also that in the breath diagram of Fig. 12, the normal breath cycles are manifested as single peaks, whereas when the volunteer breaths intensively (with an elongated thoracic perimeter), such single peaks are transformed to double peaks. This is explained by the fact that tag displacement extends beyond the quasi-linear operation range (reduced to 3 cm with the system of Fig. 10, as indicated). Nevertheless, the respiration rate can be easily retrieved from the time lapse between the minima in the breath diagram. Let us also mention that, depending on how the subject beaths (how deep), and also depending on his/her thorax diameter, the measured phases (more specifically their variation) are expected to be different. Nevertheless, this is not an issue, as far as the determination of the breath rate requires only the measurement of the period in the breath diagram.

V. Comparative analysis

As mentioned before, there are few displacement sensors based on phase variation. In [31], one of the designed and

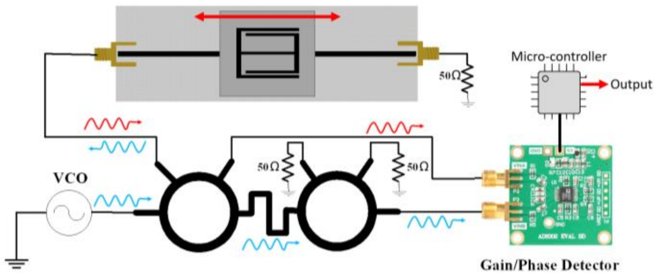

Fig. 10. Sketch of the sensor system to retrieve the phase without the use of a VNA.

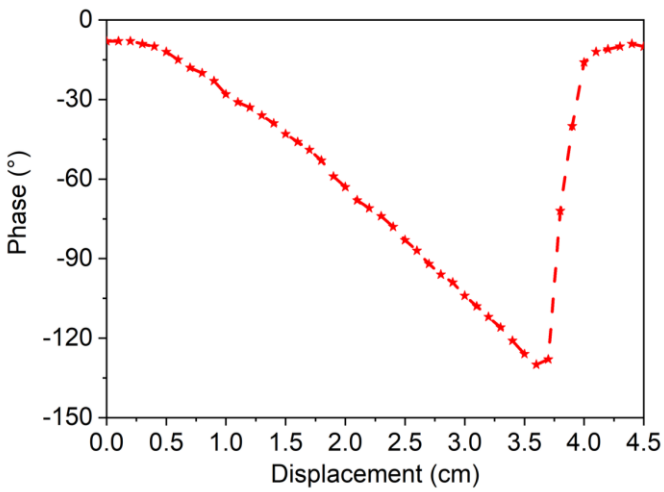

Fig. 11. Variation of the phase of the reflection coefficient with the displacement as inferred with the system of Fig. 10, using the linear displacement system available in our laboratory.

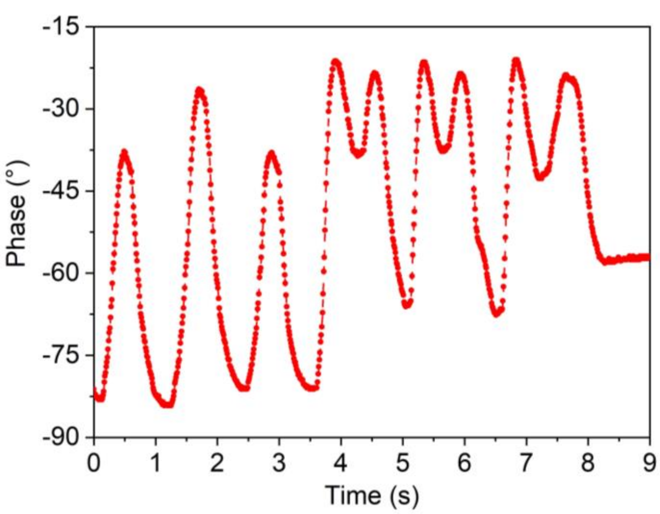

Fig. 12. Phase of the reflection coefficient recorded using the system of Fig. 10 while a volunteer with the belt-based sensor mounted on its thorax breaths.

fabricated phase-variation linear displacement sensors (operating in reflection mode) exhibits a maximum sensitivity of 313º/mm, but the device is highly non-linear (i.e., it was designed in order to detect very small changes of position of the movable part, a dielectric slab). By contrast, the sensitivity in the proposed displacement sensor is smaller (8.2 º/mm), but the linearity is good, since the reader line is matched to the reference impedance of the port ($Z_0 = 50\ \Omega$).

Concerning the input dynamic range, in the proposed sensor the input span is restricted to a range that generates a phase variation in the reader (reflection coefficient) within a cycle (2π). By this means, we avoid any phase ambiguity, and the position can be determined absolutely within that displacement span. Nevertheless, if we set a reference (REF) position value, the periodicity (repeatability) of the output variable does not represent an issue in regard to the discrimination of the resonator position. Thus, in this sense, the input dynamic range is dictated by the length of the reader line. By contrast, in most linear displacement sensors based on coupling modulation [5]-[8], or frequency variation [2], [3], where a reader line is loaded with a sensing resonator etched or printed in an independent substrate in relative motion, the input dynamic ranges are of the order of resonator dimensions, i.e., very limited. Table I reports various linear displacement sensors, where relevant parameters are included.

Table I contains also various linear electromagnetic encoders, a type of displacement and velocity sensors where the input dynamic range is given by the encoder length. In these systems, the encoders contain at least a chain of metallic or dielectric inclusions that must displace transversely over the reader line at short distance. The main difference between electromagnetic encoders and the displacement sensor system reported in this work is that electromagnetic encoders are based on pulse counting, similar to optical encoders. Thus, in such encoders, rather than the sensitivity, the relevant parameter is the spatial resolution, dictated by the period of the inclusions. In the proposed, system, if we consider that 5º in the phase of the reflection coefficient can be reliably resolved, the corresponding resolution is found to be about 0.61 mm, a very competitive value (in the case measured with VNA). Nevertheless, this resolution can be improved by increasing the operating frequency, since this boosts up the sensitivity.

TABLE I
COMPARISON OF VARIOUS LINEAR DISPLACEMENT SENSORS

Ref.	Sensitivity	Resolution (mm)	Dynamic range (cm)
[2]	110MHzmm^{-1}	0.03	0.4
[3]	80MHzmm^{-1}	< 1	0.3
[5]	95 dB/mm	< 0.05	0.06
[6]	83 dB/mm	< 0.05	0.06
[7]	25 dB/mm	< 0.2	0.1
[8]	26 dB/mm	< 0.1	0.07
[31]	313 ˚/mm	0.016	0.5
[37]	---	0.6	> 6
[38]	---	3.4	> 17
[40]	---	4.0	> 7
[44]	---	4.0	> 19
[45]	---	2.0	> 4
[46]	---	3.0	> 1.2
T.W.	**8.0 ˚/mm**	**0.61**	**4.4**

The main conclusion in this comparison is that the proposed displacement sensor exhibits good combination of linearity, dynamic range, and resolution, Moreover, the design of the sensor is very simple, since it merely consist of a transmission line terminated with a matched load fed by a harmonic signal (the reader), and an ELC resonator etched, or printed, on a movable substrate (the tag). This simplicity has been instrumental for the application of this sensor concept to the implementation of a breath rate monitoring system based on the relative displacement between the reader and the tag caused by inspiration and expiration, and achieved by conveniently designing an *ad hoc* sensor belt, as discussed in the previous section. Let us next compare the proposed breath rate sensor with other similar sensors reported in the literature.

Researchers have tried to record the breath rate using various methods and strategies. One of the commercially available and accepted methods is to use the air flow of the respiration to rotate a turbine mounted on a mask [56]. Although this breath rate monitoring method is very reliable, it is very annoying to continuously wear a mask, and hence it is not very appropriate for long term breath rate monitoring. There are also camera-based and image processing methods to retrieve the breath rate, but such techniques are very costly and cannot be used in all situations [57]. Some other researchers have tried to record the breath rate utilizing the movement of the chest. Some of these works are based on the lateral movement or stretch of a sensitive structure (capacitive, inductive, etc.) fixed on the chest or abdomen caused by the changes in the thorax's diameter during respiration [58-60]. Some others are based on the movement of the chest or abdomen along the axis normal to the chest like [61-62]. The main disadvantage of the first category is their nonlinear response and the need of making one sensor specifically for one person. For example, in [58] the authors have proposed a T-shirt with the sensor integrated on it. So, for different persons, different sensor-mounted T-shirts according to their size are needed. On the other hand, the main drawback of the second category is that the movements of the chest due to respiration can be easily confused with other movements of the person. In the system proposed in this paper, the sensor has been mounted on a belt making its usage very comfortable and easy for long term, the system is very simple and low cost, and the response has a very good linearity. Furthermore, the signal recorded as breathing rate, is very stable during the movements of persons' body. Radar-based systems constitute another category of breath rate monitoring systems [63]. Although such systems can measure the breath rate with good accuracy, the main disadvantage is the need to proper positioning the subject under study with regard to the Radar antennas (a limitation not present in the proposed system).

VI. Conclusions

In conclusion, a novel type of microwave displacement sensor has been proposed. The sensor is based on a static part (reader), a microstrip line terminated with a matched load, and a movable part (tag), an ELC resonator etched in a microwave substrate, in relative motion with regard to the axis of the reader line. By feeding the reader line with a harmonic signal tuned to the resonance frequency of the ELC resonator, the phase of the reflection coefficient of the reader line (the output variable) varies roughly linearly with the distance between the resonator position and the input port, and hence that position can be retrieved. The proposed sensor exhibits good linearity and dynamic range, as compared to other frequency-variation or coupling-modulation linear displacement sensors based on planar microwave technologies. The resolution is also good, and better than that of most reported linear electromagnetic encoders (a type of motion sensors based on multiple tag inclusions and pulse counting). The sensor has been found to be appropriate for application in breath rate monitoring. For that purpose, we have implemented an *ad hoc* belt-based sensor, in a specific arrangement that is able to provide the respiration rate from the relative periodic variation of the position between the reader and the tag generated from expiration and inspiration. This breath rate belt-based sensor has been experimentally validated, and it has been found to be a competitive approach to other breath rate monitoring sensors reported in the available literature.

References

[1] F. Martín, P. Vélez, J. Muñoz-Enano, L. Su, *Planar Microwave Sensors*, Wiley/IEEE Press, Hoboken, NJ, USA, 2022.

[2] C. Mandel, B. Kubina, M. Schüßler and R. Jakoby, "Passive chipless wireless sensor for two-dimensional displacement measurement," *2011 41st European Microwave Conference*, Manchester, UK, 2011, pp. 79-82.

[3] A. K. Horestani, J. Naqui, Z. Shaterian, D. Abbott, C. Fumeaux, and F. Martín, "Two-Dimensional Alignment and Displacement Sensor based on Movable Broadside-coupled Split Ring Resonators", *Sens. Act. A*, vol. 210, pp. 18-24, Apr. 2014.

[4] A. K. Jha, N. Delmonte, A. Lamecki, M. Mrozowski and M. Bozzi, "Design of Microwave-Based Angular Displacement Sensor," *IEEE Microw. Wireless Compon. Lett*., vol. 29, no. 4, pp. 306-308, Apr. 2019.

[5] J. Naqui, M. Durán-Sindreu, and F. Martín, "Novel sensors based on the symmetry properties of split ring resonators (SRRs)," *Sensors*, vol 11, pp. 7545–7553, 2011.

[6] J. Naqui, M. Durán-Sindreu, and F. Martín, "Alignment and position sensors based on split ring resonators," *Sensors*, vol. 12, pp. 11790–11797, 2012.

[7] A. Karami-Horestani, C. Fumeaux, S. F. Al-Sarawi, and D. Abbott, "Displacement sensor based on diamond-shaped tapered split ring resonator," *IEEE Sensors J*., vol. 13, no. 4, pp. 1153–1160, Apr. 2013.

[8] A. K. Horestani, J. Naqui, D. Abbott, C. Fumeaux, and F. Martín, "Two-dimensional displacement and alignment sensor based on reflection coefficients of open microstrip lines loaded with split ring resonators," *Electron Lett*., vol. 50, no. 8, pp. 620–622, Apr. 2014.

[9] A. K. Horestani, D. Abbott, and C. Fumeaux, "Rotation sensor based on horn-shaped split ring resonator," *IEEE Sens. J*., vol. 13, pp. 3014–3015, 2013.

[10] J. Naqui and F. Martín, "Transmission lines loaded with bisymmetric resonators and their application to angular displacement and velocity sensors," *IEEE Trans. Microw. Theory Techn*., vol. 61, no. 12, pp. 4700–4713, Dec. 2013.

[11] J. Naqui and F. Martín, "Angular displacement and velocity sensors based on electric-LC (ELC) loaded microstrip lines," *IEEE Sensors J*., vol. 14, pp. 939–940, Apr. 2014.

[12] J. Naqui, J. Coromina, A. Karami-Horestani, C. Fumeaux, and F. Martín, "Angular displacement and velocity sensors based on coplanar waveguides (CPWs) loaded with S-shaped split ring resonator (S-SRR)," *Sensors*, vol. 15, pp. 9628–9650, 2015.

[13] C. Damm, M. Schussler, M. Puentes, H. Maune, M. Maasch and R. Jakoby, "Artificial transmission lines for high sensitive microwave sensors," *IEEE Sensors Conf.*, Christchurch, New Zealand, pp.755−758, Oct. 2009.

[14] F.J. Ferrández-Pastor, J.M. García-Chamizo and M. Nieto-Hidalgo, "Electromagnetic differential measuring method: application in microstrip sensors developing", Sensors, vol. 17, p. 1650, 2017.

[15] J. Muñoz-Enano, P. Vélez, M. Gil, F. Martín, "An analytical method to implement high sensitivity transmission line differential sensors for dielectric constant measurements", *IEEE Sensors J.*, vol. 20, pp. 178-184, Jan. 2020.

[16] M. Gil, P. Vélez, F. Aznar, J. Muñoz-Enano, and F. Martín, “Differential sensor based on electro-inductive wave (EIW) transmission lines for dielectric constant measurements and defect detection”, *IEEE Trans. Ant. Propag*., vol. 68, pp. 1876-1886, Mar. 2020.

[17] J. Muñoz-Enano, P. Vélez, M. Gil, J. Mata-Contreras, and F. Martín, “Differential-mode to common-mode conversion detector based on rat-race couplers: analysis and application to microwave sensors and comparators”, *IEEE Trans. Microw. Theory Techn*., vol. 68, pp. 1312-1325, Apr. 2020.

[18] J. Coromina, J. Muñoz-Enano, P. Vélez, A. Ebrahimi, J. Scott, K. Ghorbani, F. Martín, "Capacitively-Loaded Slow-Wave Transmission Lines for Sensitivity Improvement in Phase-Variation Permittivity Sensors", *50th Europ. Microw. Conf*., Utrecht, The Netherlands Sep. 2020.

[19] A. Ebrahimi, J. Coromina, J. Muñoz-Enano, P. Vélez, J. Scott, K. Ghorbani, and F. Martín, "Highly Sensitive Phase-Variation Dielectric Constant Sensor Based on a Capacitively-Loaded Slow-Wave Transmission Line," *IEEE Trans. Circ. Syst. I: Reg. Papers*, vol. 68, no. 7, pp. 2787-2799, Jul. 2021.

[20] L. Su, J. Muñoz-Enano, P. Vélez, P. Casacuberta, M. Gil, F. Martín, “Phase-Variation Microwave Sensor for Permittivity Measurements Based on a High-Impedance Half-Wavelength Transmission Line,” *IEEE Sensors J*., vol. 21, no. 9, pp. 10647-10656, May 2021.

[21] J. Muñoz-Enano, P. Vélez, L. Su, M. Gil, P. Casacuberta, and F. Martín, “On the sensitivity of reflective-mode phase variation sensors based on open-ended stepped-impedance transmission lines: theoretical analysis and experimental validation”, *IEEE Trans. Microw. Theory Techn*. vol. 69, no. 1, pp. 308-324, Jan. 2021.

[22] L. Su, J. Muñoz-Enano, P. Velez, P. Casacuberta, M. Gil and F. Martin, "Highly Sensitive Phase Variation Sensors Based on Step-Impedance Coplanar Waveguide (CPW) Transmission Lines," *IEEE Sensors J*., vol. 21, no. 3, pp. 2864-2872, Feb. 2021.

[23] P. Casacuberta, J. Muñoz-Enano, P. Vélez, L. Su, M. Gil, and F. Martín, "Highly sensitive reflective-mode detectors and dielectric constant sensors based on open-ended stepped-impedance transmission lines", *Sensors*, vol. 20, paper 6236, 2020.

[24] L. Su, J. Muñoz-Enano, P. Vélez, M. Gil, P. Casacuberta, and F. Martín, “Highly sensitive reflective-mode phase-variation permittivity sensor based on a coplanar waveguide (CPW) terminated with an open complementary split ring resonator (OCSRR),” *IEEE Access*, vol. 9, pp. 27928-27944, 2021.

[25] P. Casacuberta, P. Vélez, J. Muñoz-Enano, L. Su, M. Gil, A. Ebrahimi and F. Martín, “Circuit analysis of a Coplanar waveguide (CPW) terminated with a step-impedance resonator (SIR) for highly sensitive one-port permittivity sensing,” *IEEE Access*, vol. 10, pp. 62597-62612, 2022.

[26] P. Casacuberta, P. Vélez, J. Muñoz-Enano, L. Su, and F. Martín "Highly sensitive reflective-mode phase-variation permittivity sensors using coupled line sections", *IEEE Trans. Microw. Theory Techn*., doi: 10.1109/TMTT.2023.3234272.

[27] P. Casacuberta, P. Vélez, J. Muñoz-Enano, L. Su, M. Gil-Barba, and F. Martín, "Reflective-Mode Phase-Variation Permittivity Sensors Based on Coupled Resonators", *IEEE Sensors 2022*, Dallas, Texas, USA, Oct. 30 - Nov. 2, 2022.

[28] M. Elgeziry, F. Paredes, P. Vélez, F. Costa, S. Genovesi, F. Martín, "A Method to Retrieve the Output Variables in Reflective-Mode Phase-Variation Sensors", *52nd Europ. Microw. Conf*., Milan, Italy, 20-25 Sep. 2022.

[29] P. Vélez, F. Paredes, P. Casacuberta, M. Elgeziry, L. Su, J. Muñoz-Enano, F. Costa, S. Genovesi, and F. Martín, "Portable Reflective-Mode Phase-Variation Microwave Sensor Based on a Rat-Race Coupler Pair and Gain/Phase Detector for Dielectric Characterization", *IEEE Sensors J*., vol. 23, no. 6, pp. 5745-5756, Mar. 2023.

[30] L. Su, P. Vélez, P. Casacuberta, J. Muñoz-Enano, M. Gil, and F. Martín, "Reflective-Mode Phase-Variation Submersible Sensor for Liquid Characterization", *IEEE Trans. Instrum. Meas*., submitted.

[31] J. Muñoz-Enano, P. Vélez, L. Su, M. Gil, and F. Martín, “A reflective-mode phase-variation displacement sensor”, *IEEE Access*, vol. 8, pp. 189565-189575, Oct. 2020.

[32] A. K. Jha, A. Lamecki, M. Mrozowski, and M. Bozzi, “A highly sensitive planar microwave sensor for detecting direction and angle of rotation,” *IEEE Trans. Microw. Theory Techn*., vol. 68, no. 4, pp. 1598–1609, Apr. 2020.

[33] A. K. Horestani, Z. Shaterian and F. Martín, "Rotation Sensor Based on the Cross-Polarized Excitation of Split Ring Resonators (SRRs)", *IEEE Sensors J*., vol 20, pp. 9706-9714, Sep. 2020.

[34] Z. Mehrjoo, A. Ebrahimi, G. Beziuk, F. Martín, and K. Ghorbani, “Microwave Rotation Sensor Based on Reflection Phase in Transmission Lines Terminated with Lumped Resonators”, *IEEE Sensors J*., doi: 10.1109/JSEN.2023.3236638.

[35] J. Mata-Contreras, C. Herrojo, and F. Martín, "Application of split ring resonator (SRR) loaded transmission lines to the design of angular displacement and velocity sensors for space applications", *IEEE Trans. Microw. Theory Techn*., vol. 65, no. 11, pp. 4450-4460, Nov. 2017.

[36] J. Mata-Contreras, C. Herrojo, and F. Martín, "Detecting the rotation direction in contactless angular velocity sensors implemented with rotors loaded with multiple chains of split ring resonators (SRRs)", *IEEE Sensors J*., vol.18, no. 17, pp. 7055-7065, Sep. 2018.

[37] C. Herrojo, F. Paredes, and F. Martín, “Double-stub loaded microstrip line reader for very high data density microwave encoders”, *IEEE Trans. Microw. Theory Techn.*, vol.67, no. 9, pp. 3527-3536, Sep. 2019.

[38] C. Herrojo, F. Paredes, and F. Martín, “3D-printed high data-density electromagnetic encoders based on permittivity contrast for motion control and chipless-RFID”, *IEEE Trans. Microw. Theory Techn*., vol. 68, no. 5, pp. 1839-1850, May 2020.

[39] C. Herrojo, F. Paredes, and F. Martín “3D-printed all-dielectric electromagnetic encoders with synchronous reading for measuring displacements and velocities”, *Sensors*, vol. 20, p. 4837, 2020.

[40] F. Paredes, C. Herrojo, F. Martín, "Microwave Encoders with Synchronous Reading and Direction Detection for Motion Control Applications", *2020 IEEE-MTT-S Int. Microw. Symp.* (IMS'20), Los Angeles, CA, USA, 21-26 Jun., 2020.

[41] C. Herrojo, F. Paredes, and F. Martín “Synchronism and Direction Detection in High-Resolution/High-Density Electromagnetic Encoders”, *IEEE Sensors J*., vol. 21, no. 3, pp. 2873-2882, Feb. 2020.

[42] F. Paredes, C. Herrojo, F. Martín, “Position sensors for industrial applications based on electromagnetic encoders”, *Sensors*, vol. 21, pp. 2738 (28 pages), 2021.

[43] F. Paredes, C. Herrojo, F. Martín, “3D-printed quasi-absolute electromagnètic encoders for chipless-RFID and motion control applications”, *Electronics*, vol. 10, paper 1154, 2021.

[44] F. Paredes, C. Herrojo, A. Moya, M. Berenguel-Alonso, D. Gonzalez, J. Bruguera, C. Delgado-Simao, and F. Martín, “Electromagnetic Encoders Screen-Printed on Rubber Belts for Absolute Measurement of Position and Velocity”, *Sensors*, vol. 22, paper 2044, 2022.

[45] A. Karami-Horestani, F. Paredes and F. Martín, “Frequency-coded and programmable synchronous electromagnètic encoders based on linear strips”, *IEEE Sensors Lett*., vol. 6, no. 8, pp. 1-4, Art. no. 3501704, Aug. 2022.

[46] A. Karami-Horestani, F. Paredes and F. Martín, “High data density absolute electromagnètic encoders based on hybrid time/frequency domain encoding”, *IEEE Sensors J*., vol. 22, no. 24, pp. 23866-23876, Dec. 2022.

[47] F. Paredes, A. Moya, M. Berenguel-Alonso, D. Gonzalez, J. Bruguera, C. Delgado-Simao, and F. Martín, “Motion Control System for Industrial Scenarios Based on Electromagnetic Encoders”, *IEEE Trans. Instrum.* Meas., vol. 72, pp. 1-12, 2023, Art no. 2003612.

[48] C.-H. Chio, R. Gómez-García, L. Yang, K.-W. Tam, W.-W. Choi, and S.-K. Ho, “An angular displacement microwave sensor using an unequal-length-bi-path transversal filtering section,” *IEEE Sensors J*., vol. 20, no. 2, pp. 715–722, Jan.2020.

[49] C.-H. Chio, R. Gómez-García, . Yang, K.-W. Tam, W.-W. Choi, and S.-K. Ho, “Directional-coupler-based microwave sensors for differential angular displacement measurement,” *Int. J. RF Microw. Comput.-Aid. Eng*., p. e22338, Jun. 2020.

[50] C.-H. Chio, R. Gómez-García, L. Yang, K. W. Tam, W.-W. Choi, and S. K. Ho, “An angular displacement sensor based on microwave transversal signal interference principle,” *IEEE Sensors J*., vol. 20, no. 19, pp. 11237–11246, Oct. 2020.

[51] C.-H. Chio, K.-W. Tam, and R. Gómez-García, “Filtering Angular Displacement Sensor Based on Transversal Section with Parallel-Coupled-Line Path and U-shaped coupled slotline,” *IEEE Sensors J*., vol. 22, no. 2, pp. 1218-1226, Jan. 2022.

[52] D. Schurig, J. J. Mock, and D. R. Smith, “Electric-field-coupled resonators for negative permittivity metamaterials,” *Appl. Phys. Lett*., vol. 88, paper 041109, 2006.

[53] F. Martín, *Artificial Transmission Lines for RF and Microwave Applications*, John Wiley, Hoboken, NJ, USA, 2015.

[54] L. Su, J. Muñoz-Enano, P. Vélez, J. Martel, F. Medina, and F. Martín, "On the modelling of microstrip lines loaded with dumbbell defect-ground-structure (DB-DGS) and folded DB-DGS resonators", *IEEE Access*, vol. 9, pp. 150878-150888, 2021.

[55] D. M. Pozar, *Microwave Engineering*, 4th Ed., John Wiley, Hoboken, NJ, USA, 2011.

[56] Y. Sokol, R. Tomashevsky and K. Kolisnyk, "Turbine spirometers metrological support", *2016 International Conference on Electronics and Information Technology (EIT)*, pp. 1-4, May 2016.

[57] C. Massaroni, E. Schena, S. Silvestri and S. Maji, "Comparison of two methods for estimating respiratory waveforms from videos without contact", *2019 IEEE International Symposium on Medical Measurements and Applications (MeMeA)*, pp. 1-6, Jun. 2019.

[58] M. el Gharbi, R. Fernandez-Garcia, and I. Gil, "Embroidered wearable antenna-based sensor for real-time breath monitoring," *Measurement*, vol. 195, p. 111080, 03 2022.

[59] S. K. Kundu, S. Kumagai and M. Sasaki, "A Wearable Capacitive Sensor for Monitoring Human Respiratory Rate", *Japanese Journal of Applied Physics*, vol. 52, no. 4S, pp. 04CL05, Apr. 2013.

[60] C. F. Clarenbach, O. Senn, T. Brack, M. Kohler and K. E. Bloch, "Monitoring of ventilation during exercise by a portable respiratory inductive plethysmograph", *Chest*, vol. 128, no. 3, pp. 1282-1290, Sep. 2005.

[61] M. Elgeziry, F. Costa, A. Tognetti and S. Genovesi, "Wearable Chipless Sensor for Breath Rate monitoring," *2022 3rd URSI Atlantic and Asia Pacific Radio Science Meeting (AT-AP-RASC)*, Gran Canaria, Spain, 2022, pp. 1-4, doi: 10.23919/AT-AP-RASC54737.2022.9814232.

[62] M. Elgeziry, F. Costa, A. Tognetti and S. Genovesi, "Wearable Sensor for Breath Rate Monitoring," *2022 16th European Conference on Antennas and Propagation (EuCAP)*, Madrid, Spain, 2022, pp. 1-5, doi: 10.23919/EuCAP53622.2022.9769206.

[63] F. Yang, Z. He, Y. Fu, L. Li, K. Jiang and F. Xie, "Noncontact Detection of Respiration Rate Based on Forward Scatter Radar", *Sensors*, vol. 19, no. 21, pp. 4778, Jan. 2019.

Amirhossein Karami Horestani has got his bachelor degree at 2015 in the field of biomedical engineering from the University of Isfahan. Then he studies at the University of Tehran in the field of micro/nano electronics for the master's degree until 2018. Since December 2021 he is working on microwave sensors and near-field RFID systems as a PhD student at Universitat Autònoma de Barcelona.

Ferran Paredes (M'14-SM'22) received the Telecommunications Engineering degree from the Universitat Autònoma de Barcelona in 2006 and the PhD degree in Electronics Engineering from the same university in 2012. He is working as a Research Assistant at the Universitat Autònoma de Barcelona and his research interests include metamaterial concepts, passive microwaves devices, antennas, and RFID.

Ferran Martín (M'04-SM'08-F'12) was born in Barakaldo (Vizcaya), Spain in 1965. He received the B.S. Degree in Physics from the Universitat Autònoma de Barcelona (UAB) in 1988 and the PhD degree in 1992. From 1994 up to 2006 he was Associate Professor in Electronics at the Departament d'Enginyeria Electrònica (Universitat Autònoma de Barcelona), and since 2007 he is Full Professor of Electronics. In recent years, he has been involved in different research activities including modelling and simulation of electron devices for high frequency applications, millimeter wave and THz generation systems, and the application of electromagnetic bandgaps to microwave and millimeter wave circuits. He is now very active in the field of metamaterials and their application to the miniaturization and optimization of microwave circuits and antennas. Other topics of interest include microwave sensors and RFID systems, with special emphasis on the development of high data capacity chipless-RFID tags. He is the head of the Microwave Engineering, Metamaterials and Antennas Group (GEMMA Group) at UAB, and director of CIMITEC, a research Center on Metamaterials supported by TECNIO (Generalitat de Catalunya). He has organized several international events related to metamaterials and related topics, including Workshops at the IEEE International Microwave Symposium (years 2005 and 2007) and European Microwave Conference (2009, 2015 and 2017), and the Fifth International Congress on Advanced Electromagnetic Materials in Microwaves and Optics (Metamaterials 2011), where he acted as Chair of the Local Organizing Committee. He has acted as Guest Editor for six Special Issues on metamaterials and sensors in five International Journals. He has authored and co-authored over 650 technical conference, letter, journal papers and book chapters, he is co-author of the book on Metamaterials entitled *Metamaterials with Negative Parameters: Theory, Design and Microwave Applications* (John Wiley & Sons Inc.), author of the book *Artificial Transmission Lines for RF and Microwave Applications* (John Wiley & Sons Inc.), co-editor of the book *Balanced Microwave Filters* (Wiley/IEEE Press), co-author of the book *Time-Domain Signature Barcodes for Chipless-RFID and Sensing Applications* (Springer), and co-author of the book *Planar Microwave Sensors* (Wiley/IEEE Press). Ferran Martín has generated 22 PhDs, has filed several patents on metamaterials and has headed several Development Contracts.

Prof. Martín is a member of the IEEE Microwave Theory and Techniques Society (IEEE MTT-S). He is reviewer of the IEEE Transactions on Microwave Theory and Techniques and IEEE Microwave and Wireless Components Letters, among many other journals, and he serves as member of the Editorial Board of IET Microwaves, Antennas and Propagation, International Journal of RF and Microwave Computer-Aided Engineering, and Sensors. He is also a member of the Technical Committees of the European Microwave Conference (EuMC) and International Congress on Advanced Electromagnetic Materials in Microwaves and Optics (Metamaterials). Among his distinctions, Ferran Martín has received the 2006 Duran Farell Prize for Technological Research, he holds the *Parc de Recerca UAB – Santander* Technology Transfer Chair, and he has been the recipient of three ICREA ACADEMIA Awards (calls 2008, 2013 and 2018). He is Fellow of the IEEE and Fellow of the IET.